Acta Cryst. (1985). B41, 113-122

Alloxan – Electrostatic Properties of an Unusual Structure from X-ray and Neutron Diffraction

BY S. SWAMINATHAN AND B. M. CRAVEN

Department of Crystallography, University of Pittsburgh, Pittsburgh, PA 15260, *USA*

AND R. K. MCMULLAN

Department of Chemistry, Brookhaven National Laboratory, Upton, NY 11973, *USA*

(*Received* 9 *April* 1984; *accepted* 24 *July* 1984)

Abstract

The crystal structure of alloxan [2,4,5,6(1*H*,3*H*)-pyrimidinetetrone, $C_4H_2N_2O_4$, $M_r = 142{\cdot}07$, tetragonal, space group $P4_12_12$, $Z = 4$] has been determined from neutron diffraction data ($\sin\theta/\lambda < 0{\cdot}78$ Å^{-1}) at 42 and 123 K and from X-ray diffraction data ($\sin\theta/\lambda < 1{\cdot}15$ Å^{-1}) at 123 K. [X-ray crystal data at 123 K: $a = 5{\cdot}850\,(1)$, $c = 13{\cdot}915\,(3)$ Å, $V = 476{\cdot}2$ Å^3, $D_x = 1{\cdot}98$ g cm^{-3}, $\mu = 1{\cdot}66$ cm^{-1}, $F(000) = 288$, $R(F) = 0{\cdot}043$ for 1097 reflections with $F_o > 2\sigma$.] Alloxan has an unusually high crystal density (1·93 g cm^{-3} at 295 K), apparently due to short intermolecular O=C···O distances (2·73 Å at 123 K). There is no H-bonding except for a weak bifurcated interaction with long H···O distances (2·32, 2·35 Å) at 123 K. Bond lengths and angles from neutron diffraction (corrected for thermal motion) have e.s.d.'s less than 0·002 Å and 0·1°. They indicate that the effects of conjugation in alloxan are small. With fixed values for all nuclear positional and thermal parameters as determined by neutron diffraction, the X-ray data were used to determine the charge-density distribution assuming Stewart's rigid pseudoatom model. The resulting electron population parameters were also used to map the electrostatic potential for an isolated molecule and for a selected group of molecules removed from the lattice. Electrostatic properties show the bifurcated H-bond to be weakly attractive. In the carbonyl groups, electron density at the C atom is depleted from both sides of the molecular plane, thus deshielding the atomic nucleus. Although the shortest intermolecular C···O distances are formed with O atoms carrying a small negative charge, −0·11 (3)e, these interactions are weak. It appears that the van der Waals radius for carbonyl C atoms should be smaller than for aromatic C atoms by at least 0·2 Å.

Introduction

Alloxan (Fig. 1) is remarkable for its high crystal density (1·93 g cm^{-3} at 295 K). The crystal structure (Bolton, 1964*a*) consists of a herringbone packing of nearly planar molecules with unusually short intermolecular distances O=C···O involving carbonyl groups [2·79 Å at 295 K, Bolton (1964*a*); see also Fig. 2]. The nature of these interactions in alloxan and several other crystal structures is not well understood (Bolton, 1964*b*; Pullman, 1964; Prout & Wallwork, 1966; Bürgi, Dunitz & Shefter, 1974). Another remarkable feature of the alloxan structure is the absence of conventional H-bonding, although the molecule consists entirely of potential N–H donor and C=O acceptor groups. There appear to be weak bifurcated H-bonding interactions (Fig. 3), but these involve H···O distances (2·32, 2·35 Å at 123 K) which are almost as long as van der Waals distances.

Our X-ray and neutron diffraction study of alloxan at 123 K was undertaken for a better understanding of the intermolecular interactions in terms of the electrostatic properties of the molecule. A second neutron data set at a lower temperature (42 K) was collected to obtain more details concerning the molecular thermal motion in the crystal.

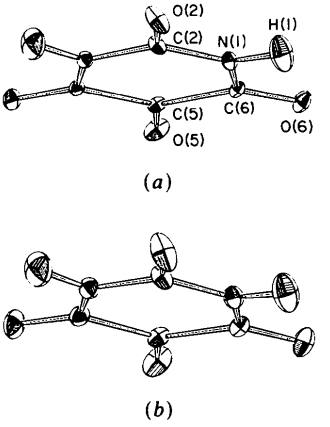

Fig. 1. Alloxan, atomic nomenclature and thermal ellipsoids at 50% probability as determined by neutron diffraction. A crystallographic twofold axis passes through atoms O(2), C(2), C(5) and O(5). (*a*) 42 K, (*b*) 123 K.

0108-7681/85/020113-10$01.50

Experimental

The structure determination at 42 and 123 K from neutron diffraction

Commercially available alloxan, so-called alloxan monohydrate, is 5,5-dihydroxybarbituric acid (Singh, 1960; Mootz & Jeffrey, 1965). Anhydrous alloxan [2,4,5,6(1*H*,3*H*)-pyrimidinetetrone] was obtained (after Bolton, 1964*a*) by heating a sample from Eastman Kodak Co., to 483 K at low pressure (~1·3 kPa) and then subliming in a sealed system at 503 K overnight. Transparent lemon-yellow crystals obtained in this way react with atmospheric moisture. However, anhydrous crystals can be preserved for long periods by lightly coating them with clear varnish.*

Alloxan crystallizes in the tetragonal space group $P4_12_12$, with four molecules of $C_4H_2N_2O_4$ per cell in positions with twofold crystallographic symmetry (Bolton, 1964*a*). The crystal selected for neutron data collection exhibited the forms {001}, {120} with volume 4·29 mm^3 as determined with an optical microscope, and had a weight 8·29 mg. Thus the crystal density 1·93 g cm^{-3} at room temperature agrees with the value 1·93 g cm^{-3} determined by flotation (Bolton, 1964*a*).

The neutron data were collected at the Brookhaven High Flux Beam Reactor with a beam monochromated by reflection from Be(002) planes. The wavelength [1·0470 (1) Å] was determined using reflections from a standard KBr crystal (a_0 = 6·6000 Å at 298 K).

The crystal was mounted with the [210] axis nearly coincident with the φ axis of a four-circle diffractometer and was attached with rubber cement to a hollow Al pin enclosed in an Al can filled with He gas; cooling was by means of a closed-cycle refrigerator.* Unit-cell parameters (Table 1) were determined by least-squares fitting of $\sin^2\theta$ values for 32 reflections with $50 < 2\theta < 56°$.

After cooling at ~1° min^{-1}, neutron diffraction data were collected at 123 K.† Integrated intensities were measured for reflections in an octant of reciprocal space by $\omega/2\theta$ step scans, with scan width $\Delta 2\theta = 3·2°$ for $\sin\theta/\lambda < 0·48$ Å^{-1} and $\Delta 2\theta = (2·78 + 0·498\tan\theta)°$ for $0·48 < \sin\theta/\lambda < 0·78$ Å^{-1}. Backgrounds were estimated from the first and last tenths of each scan and variances were assumed to be $\sigma^2(I) = \sigma_c^2 + (0·02I)^2$, where σ_c^2 was the variance due to counting statistics. The intensities of two check reflections were constant within 2%. Absorption corrections were applied using an analytical procedure (de Meulenaer & Tompa, 1965; Templeton & Templeton, 1973) with μ = 0·70 cm^{-1} calculated by assuming 2·48 m^2 kg^{-1} for the mass absorption of bonded H atoms (McMullan & Koetzle, 1980). Intensities of equivalent *hkl* and *khl* reflections were averaged (R_w = 0·012 for 498 pairs), giving 614 reflections for the structure refinement.

Crystal cooling at ~1° min^{-1} was resumed with the aim of collecting another data set at ~10 K. However, between 40 and 30 K, a 30% decrease was observed in the peak intensity of the check reflection (114). The change was found to be reversible and to occur at 34·5 K. For several other reflections, ω scans showed differences in profile, although $\omega/2\theta$ scans showed no effect on the integrated intensity. Because of time limitations, the possibility that alloxan undergoes a phase transition at 34·5 K was not explored in further detail.

To permit comparison with the crystal structure at higher temperatures, the second data set was collected at 42 K. Integrated intensities were measured only for the 609 reflections in the sector *hkl* with $h > k$, other experimental conditions being the same as before.

Table 1. *Crystal-lattice parameters for alloxan*

	293 K	123 K		42 K
	X-ray*	X-ray	Neutron	Neutron
a	5·886 (7) Å	5·850 (1) Å	5·850 (1) Å	5·841 (1) Å
c	14·100 (15)	13·915 (3)	13·913 (3)	13·853 (3)

* See Bolton (1964*a*); Cu $K\alpha$ radiation.

* Krylon Crystal Clear Spray, Coating No. 1302; Krylon Inc., Norristown, PA.

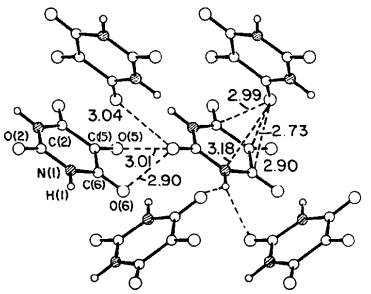

Fig. 2. The crystal structure in projection down **b**, with **c** running up the page. Atoms are represented as circles of increasing size for H, C, N, O with N atoms shaded. Intermolecular distances C···O (Å) are rounded values determined at 123 K.

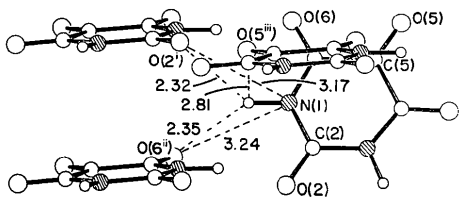

Fig. 3. The crystal environment of the N–H group. Shortest intermolecular H···O and N···O distances (Å) are rounded values determined at 123 K.

* Air Products & Chemicals, Inc. DISPLEX Model CS-202.

† The temperature was monitored by a Pt-resistance thermometer with calibration based on the magnetic phase transition of FeF_2 at 78·4 K (Hutchings, Schulhof & Guggenheim, 1972).

Structure refinements were performed with a locally modified version of *ORFLS* (Busing, Martin & Levy, 1962), minimizing $\sum w\Delta^2$, where $\Delta = (|F_o|^2 - |F_c|^2)$ and $w = \sigma^{-2}(F_o^2)$. Neutron coherent scattering lengths was taken from Koester (1977) and initial parameter values from Bolton (1964*a*). There were 58 variables consisting of a scale factor, isotropic extinction factor g (type I crystal, Lorentzian mosaicity; Becker & Coppens, 1974), and the nuclear positional and anisotropic thermal parameters. At convergence $R_w(F^2) = 0{\cdot}038$, $R(F^2) = 0{\cdot}024$, $S = 1{\cdot}15$,* $g = 0{\cdot}18\,(1) \times 10^{-4}$ rad^{-1}, maximum parameter shift/error = 0·05 for the 123 K data, and 0·048, 0·029, 1·43, $0{\cdot}16\,(1) \times 10^{-4}$ rad^{-1}, 0·05 respectively for the 42 K data. The final nuclear positional and thermal parameters are in Table 2.† Thermal ellipsoids are plotted in Fig. 1. Results of a refinement including third-order cumulants (Johnson & Levy, 1974) are not presented, since none of the c_{jkl} values was found to be significantly different from zero.

The structure determination at 123 K *from X-ray diffraction*

The alloxan crystal used for data collection measured $0{\cdot}40 \times 0{\cdot}30 \times 0{\cdot}30$ mm, exhibited the faces $(11\bar{4})$, $(\bar{1}\bar{1}4)$, $(1\bar{2}\bar{2})$, $(\bar{1}20)$, $(\bar{2}\bar{1}4)$, (100), and was mounted approximately normal to the $(\bar{1}20)$ face. Data were collected with an Enraf–Nonius CAD-4 diffractometer using Zr-filtered Mo $K\alpha$ radiation (λ = 0·7107 Å), with the crystal cooled to 123 ± 2 K by a stream of N_2 gas from an Enraf–Nonius low-temperature device. Unit-cell parameters were obtained by least-squares fit of $\sin^2\theta$ values for 50 reflections with $18° < |\pm\theta| < 26°$. There is excellent agreement between the lattice parameters obtained with X-ray and neutron diffraction (Table 1). Intensity data were measured by $\omega/2\theta$ scans recorded at 96 equal intervals, using a variable scan width $\Delta 2\theta = (2{\cdot}0 + 0{\cdot}9 \tan\theta)°$ for all reflections with $\sin\theta/\lambda < 1{\cdot}15$ Å^{-1} in a sector hkl with $h < k$. Three check reflections used for scaling gave intensity variations within 5%. Integrated intensities were estimated by the Lehmann & Larsen (1974) method as modified by Blessing, Coppens & Becker (1974). Weak reflections for which the method failed were analyzed individually from the intensity profile. The variance in an integrated intensity was assumed to be $\sigma^2(I) = \sigma_c^2 + (0{\cdot}02I)^2$, where σ_c^2 is the variance from counting statistics. From a total of 1468 reflections, 1097 with $|F_o| > 2\sigma$ were used in the structure determination. These were not corrected for X-ray absorption ($\mu = 1{\cdot}66$ cm^{-1}).

The electronic charge density in the crystal structure was determined by full-matrix least-squares refinement, assuming the rigid pseudoatom model of Stewart (1976) and using the computer programs of Craven & Weber (1981). The C, N and O pseudoatoms were assumed to have an invariant core consisting of a spherical K shell (Clementi, 1965) with X-ray scattering factors given by Stewart (1970), modified to include dispersion corrections (Cromer, Waber & Ibers, 1974).* Functions assumed for the variable valence-shell density and the corresponding

Table 2. *Atomic parameters for alloxan*

(*a*) Nuclear positional parameters ($\times 10^5$). These are from neutron diffraction, the two values being for 42 K (above) and 123 K (below).

	x	*y*	*z*
N(1)	14559 (9)	−6589 (10)	−5820 (4)
	14489 (7)	−6532 (7)	−5821 (3)
C(2)	−4680 (27)	−4680	0
	−4688 (21)	−4688	0
C(5)	29927 (26)	29927	0
	29840 (20)	29840	0
C(6)	32135 (12)	8753 (13)	−6449 (4)
	32026 (9)	8796 (10)	−6458 (3)
O(2)	−19367 (33)	−19367	0
	−19306 (27)	−19306	0
O(5)	44422 (34)	44422	0
	44318 (27)	44318	0
O(6)	48677 (17)	6297 (18)	−11651 (6)
	48473 (13)	6347 (14)	−11651 (6)
H(1)	14838 (36)	−20364 (36)	−10361 (14)
	14704 (28)	−20268 (27)	−10347 (11)

(*b*) Anisotropic thermal parameters (Å$^2 \times 10^4$). These are for temperature factors of the form $T = \exp(-2\pi^2 \sum_i \sum_j h_i h_j a_i^* a_j^* U_{ij})$. The three values are from neutron diffraction at 42 K (above), 123 K (middle), and from X-ray diffraction at 123 K [below, except for H(1)].

	U_{11}	U_{22}	U_{33}	U_{12}	U_{13}	U_{23}
N(1)	74 (2)	74 (2)	88 (2)	−4 (2)	−3 (2)	−17 (2)
	120 (2)	116 (2)	135 (1)	−3 (1)	−4 (1)	−22 (1)
	113 (5)	111 (5)	133 (4)	−2 (4)	−2 (4)	−26 (4)
C(2)	54 (5)	54	131 (4)	−10 (3)	0 (5)	0
	93 (4)	93	195 (3)	−6 (3)	5 (4)	−5
	91 (7)	91	212 (8)	−14 (6)	3 (9)	−3
C(5)	77 (5)	77	64 (3)	−31 (4)	−5 (5)	5
	127 (4)	127	95 (2)	−39 (3)	−2 (4)	2
	135 (8)	135	97 (5)	−44 (6)	5 (8)	−5
C(6)	63 (3)	93 (3)	56 (2)	−7 (2)	8 (2)	0 (2)
	109 (3)	140 (2)	95 (2)	−13 (2)	9 (2)	−1 (2)
	117 (5)	149 (6)	91 (3)	−12 (4)	15 (4)	−5 (4)
O(2)	76 (6)	76	307 (7)	−25 (4)	20 (7)	−20
	142 (5)	142	471 (6)	−54 (4)	80 (7)	−80
	153 (12)	153	476 (16)	−60 (9)	85 (19)	−85
O(5)	133 (7)	133	112 (4)	−95 (5)	−7 (7)	7
	214 (6)	214	179 (4)	−132 (5)	26 (6)	−26
	214 (11)	214	184 (8)	−131 (9)	27 (14)	−27
O(6)	91 (4)	171 (4)	96 (3)	−9 (3)	37 (3)	2 (3)
	155 (3)	244 (3)	164 (3)	−22 (3)	66 (2)	−26 (3)
	154 (6)	260 (7)	158 (5)	−19 (7)	70 (5)	−23 (6)
H(1)	236 (8)	206 (8)	292 (8)	4 (7)	−15 (7)	−139 (7)
	288 (7)	257 (7)	355 (7)	17 (6)	−20 (6)	−142 (6)

*$R_w(F^2) = (\sum w\Delta^2 / \sum wF_o^4)^{1/2}$, $R(F^2) = (\sum|\Delta| / \sum F_o^2)$, and $S = [\sum w\Delta^2/(m-n)]^{1/2}$.

†Lists of observed and calculated F^2 values [including $\sigma(F^2)$ and calculated extinction factors] for neutron data and $|F|$, $\sigma(F)$ for X-ray data, together with un-normalized electron population parameters, have been deposited with the British Library Lending Division as Supplementary Publication No. SUP39826 (24 pp.). Copies may be obtained through The Executive Secretary, International Union of Crystallography, 5 Abbey Square, Chester CH1 2HU, England.

* After the refinement, an effort was made to determine the absolute configuration of the crystal structure. For 100 reflections chosen because they were most sensitive to enantiomorphism, the least-squares residual $\sum w\Delta^2$ was found to be 176·7 for space group $P4_12_12$ and 178·0 for $P4_32_12$. This was considered to be a weak indication in favor of the assumed space group $P4_12_12$.

Table 3. *Electron population parameters* ($\times 10^2$) *for alloxan*

The values correspond to the charge-density functions given by Epstein *et al.* (1982), normalized according to Hansen & Coppens (1978) and transformed to a molecular Cartesian axial system with x along the C(2)–O(2) bond and y normal to the molecular plane.

	p_v	d_1	d_2	d_3	q_1	q_2	q_3	q_4	q_5
N(1)	550 (4)	1 (2)	2 (2)	0 (2)	1 (2)	−3 (2)	1 (2)	−2 (2)	0 (2)
C(2)	383 (6)	16 (5)	0	0	14 (4)	0	0	−4 (3)	−8 (4)
C(5)	393 (6)	2 (5)	0	0	16 (4)	0	0	−6 (3)	8 (4)
C(6)	391 (4)	−4 (2)	2 (2)	1 (2)	12 (2)	−2 (2)	1 (2)	−2 (2)	10 (2)
O(2)	604 (4)	6 (4)	0	0	−6 (3)	0	0	−2 (3)	12 (4)
O(5)	600 (4)	2 (4)	0	0	2 (3)	0	0	−6 (3)	16 (3)
O(6)	611 (3)	−2 (1)	5 (2)	−3 (1)	10 (2)	1 (2)	5 (2)	−4 (2)	−1 (2)
H(1)	66 (4)	6 (1)	3 (3)	−10 (3)	7 (3)	−5 (3)	−3 (3)	3 (4)	5 (3)

	o_1	o_2	o_3	o_4	o_5	o_6	o_7
N(1)	−2 (3)	3 (3)	4 (3)	2 (3)	24 (3)	4 (3)	6 (3)
C(2)	0 (6)	0	0	−2 (6)	−12 (6)	0	0
C(5)	4 (6)	0	0	6 (6)	22 (6)	0	0
C(6)	0 (3)	−4 (3)	−5 (4)	1 (3)	−12 (3)	1 (3)	0 (3)
O(2)	8 (6)	0	0	−6 (6)	−2 (6)	0	0
O(5)	0 (5)	0	0	2 (5)	−6 (5)	0	0
O(6)	−1 (2)	−5 (2)	−2 (2)	−3 (2)	1 (2)	−2 (2)	1 (2)

scattering factors were those listed in an Appendix by Epstein, Ruble & Craven (1982). The valence density is then given by a series of terms, each the product of a variable electron population parameter, a single Slater-type radial function and a multipole angular function. The radial exponents were assigned fixed standard values $\alpha = 3{\cdot}4, 3{\cdot}9, 4{\cdot}5$, and $2{\cdot}5$ bohr^{-1} (the Bohr radius is 52·92 pm) for C, N, O, and H pseudoatoms respectively (Hehre, Stewart & Pople, 1969). Multipole expansions were up to octopole (quadrupole for H).

In the initial refinement, the 125 variables consisted of a scale factor, an isotropic extinction parameter g (type I crystal, Lorentzian mosaicity; Becker & Coppens, 1974), 34 anisotropic thermal parameters for non-H atoms and 89 electron population parameters. The residual $\sum w\Delta^2$ was minimized, where $\Delta = |F_o| - |F_c|$ and $w = \sigma^{-2}(F_o)$. After refinement, the sum of the monopole population parameters was 25·60 (14) e, in good agreement with the net valence charge (26 e) expected for the atoms of the asymmetric unit. Accordingly, the scale factor was constrained so that the molecule would be electrostatically neutral in all further refinements. The extinction parameter was eliminated because of its marginally significant value [$g = 0{\cdot}16\,(8) \times 10^{-4}$ rad^{-1}]. The refinement was then completed, giving $R_w(F) = 0{\cdot}029$, $R(F) = 0{\cdot}043$, $S = 1{\cdot}00$, and maximum parameter shift/e.s.d. 0·70 [in q_4 for pseudoatom C(6)]. A difference Fourier synthesis (not shown) contained some possibly significant residual electron density, but these features became negligible when the map was calculated with only reflections having $\sin\theta/\lambda < 0{\cdot}7$ Å^{-1}.

The anisotropic thermal parameters from this refinement (Table 2*b*) are in very good agreement with the values obtained from neutron diffraction at 123 K. This enabled an additional refinement to be carried out in which all atoms were given fixed positional and thermal parameters determined by neutron diffraction. Thus, the X-ray diffraction data were used only for determining the 89 electron population parameters. Convergence was obtained with $R_w(F) = 0{\cdot}032$, $R(F) = 0{\cdot}045$ and $S = 1{\cdot}07$. The final difference Fourier synthesis (Fig. 4) shows some residual density, notably at the atomic centers, the most significant feature (5σ) being at the N atom. However, the model is considered to have given a very satisfactory fit to the total charge density. The pseudoatom electron population parameters from this refinement (Table 3) are the basis for the calculation and discussion of the electrostatic properties of the molecule, such as the X–N Fourier maps (Fig. 5). The maps of deformation charge density and total electrostatic potential (Figs. 6, 7, 8) were calculated for a static arrangement of pseudoatoms assuming the charge density functions of Epstein *et al.* (1982). These computations were carried out with the programs of Craven & Weber (1981) and He (1983). It should be noted that the electrostatic potential maps contain contributions from the atomic cores and nuclei.

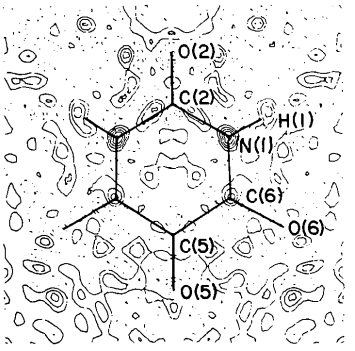

Fig. 4. Difference Fourier synthesis after least-squares refinement, showing the residual electron density in the molecular plane. Reflections with $\sin\theta/\lambda \le 1{\cdot}15$ Å^{-1} are included. Contours are at intervals of 0·10 e Å^{-3} with the zero contour omitted.

Table 4. *Rigid-body thermal-vibration tensors*

The rigid-body thermal parameters are for the molecule with H atoms omitted. They are with respect to the origin at the center of mass and a molecular Cartesian axial system with x along the C(2)–O(2) bond and y normal to the molecular plane.

	42 K			123 K		
Translation, T ($Å^2 \times 10^4$)	46 (3)	0	0	88 (3)	0	0
		68 (2)	−11 (2)		107 (3)	−16 (3)
			54 (4)			65 (4)
Libration, L (deg^2)	4·2 (4)	0	0	8·8 (4)	0	0
		5·9 (4)	−0·9 (3)		13·5 (5)	−1·1 (4)
			4·7 (3)			5·3 (3)
Cross tensor, S (deg Å $\times 10^3$)	−11 (6)	0	0	−22 (8)	0	0
	0	55 (8)	9 (5)	0	84 (11)	3 (6)
	0	27 (4)	−44	0	24 (4)	−62
Principal values for L and their direction cosines	4·4	(1, 0, 0)		8·8	(1, 0, 0)	
	7·4	(0, 0·88, −0·49)		13·7	(0, 0·99, −0·13)	
	4·1	(0, 0·49, 0·88)		5·2	(0, 0·13, 0·99)	

The molecular packing arrangement

The alloxan molecules lie on the twofold rotation axes which are parallel to the [110] face diagonals of the unit cell. The non-H atoms of each molecule are coplanar within experimental error at 295 (Bolton 1964*a*), 123 and 42 K. The best least-squares plane for these atoms has its normal with direction cosines (−0·4850, 0·4850, −0·7276) at 295 K, (−0·4819, 0·4819, −0·7318) at 123 K, (−0·4795, 0·4795, −0·7349) at 42 K (values with respect to the crystal axes). Thus the tilt of the molecule with respect to the (001) basal plane decreases slightly (43·3, 43·0, 42·7°) with decreasing temperature, in accord with the contraction of the unit cell, which is greater along c ($\Delta c/c = 0{\cdot}0178$)* than in the basal plane ($\Delta a/a = 0{\cdot}0077$). The H atoms are significantly displaced from the molecular plane [0·067 (5) Å at 123 K; 0·069 (4) Å at 42 K]. As a result, the two shortest intermolecular distances H···O(2^{i}) and H···O(6^{ii}), which would otherwise be equal, become slightly shorter and longer respectively (2·32, 2·35 Å; Fig. 3). As shown in Fig. 3, there are five O atoms within 3 Å of each H atom in alloxan, including O(2) and O(6) in the same molecule. None forms N–H···O hydrogen bonds of the usual kind. However, the atoms O(2^{i}) and O(6^{ii}) form a weak bifurcated H-bond according to the geometrical criteria proposed by Hamilton & Ibers (1968). Thus, the two H···O distances are almost 0·3 Å less than the sum of the van der Waals radii (2·6 Å; Pauling, 1960).† By comparison, the symmetric bifurcated H-bond in violuric acid monohydrate has considerably shorter H···O distances (2·07, 2·10 Å; Craven & Takei, 1964).

As shown in Fig. 2, there are three distinct intermolecular O=C···O interactions with C···O distances less than 3 Å, all involving the same O(6) atom of one molecule and three carbonyl C atoms of a second molecule. The shortest of these [C(5)···O(6); 2·79 Å at 295 K, 2·73 Å at 123 K, and 2·72 Å at 42 K] is considerably shorter than the sum of the van der Waals radii (3·1 Å; Pauling, 1960). Because of the twofold crystallographic symmetry (Fig. 7*a*), each alloxan molecule forms short C···O distances with four neighbors (see Fig. 4 in Bolton, 1964*a*), giving rise to the unusually dense molecular packing arrangement.

Molecular thermal motion; bond lengths and angles

The nuclear thermal vibrations were analyzed using the rigid-body model (Schomaker & Trueblood, 1968) in order to understand the molecular thermal motion and to estimate the corrections in bond lengths and angles. A full-matrix least-squares procedure (Craven & He, 1982) was used to minimize the residual $\sum w_k \Delta_k^2$, where Δ_k is the difference between neutron and calculated U_{ij} values for the kth atom and $w_k = \sigma^{-2}(U_k)$ is the mean square variance in U_{ij} values for the kth atom. A satisfactory fit (Table 4) was obtained when the H atoms were omitted from the rigid body ($R_w = 0{\cdot}048$, $S = 2{\cdot}20$ at 123 K; $R_w = 0{\cdot}056$, $S = 1{\cdot}61$ at 42 K). However, it was observed that for atom O(2), the calculated m.s. amplitude along the direction of greatest thermal motion (Fig. 1) was consistently small by $\sim 0{\cdot}0040$ $Å^2$ when compared with the neutron diffraction values at 42 and 123 K and the X-ray values at 123 and 295 K (Bolton, 1964*a*). The difference was attributed to a non-rigid component in the thermal motion of O(2). This seems reasonable in terms of the molecular packing, because the non-rigid vibration would be directed between two neighboring molecules.

For the H atom, m.s. amplitudes for non-rigid motion were estimated from the differences Δ_k. As expected, the values 0·0044, 0·0055 (8) $Å^2$ for N–H bond stretching and 0·0148, 0·0159 (8) $Å^2$ for in-plane

* Here $\Delta c/c = (c_{293K} - c_{42K})/c_{123K}$.

† Jeffrey & Maluszynska (1982) have proposed alternative criteria whereby H-bonding exists when the H···O distance is less than 2·85 Å and the N–H···O angle is greater than 75°. The second requirement eliminates the intramolecular H···O(2) and H···O(6) interactions, since the N–H···O angles are 67 and 64°. However, the interaction N–H···O(5^{iii}) (Fig. 3) becomes an additional weak H-bond (distance 2·81 Å, angle 91°). These authors would describe the H-bond in alloxan as a four-center interaction.

motion at 42 and 123 K show little change with temperature. However, there is a significant decrease in the out-of-plane motion from 0·0190 (7) Å^2 at 42 K to 0·0128 (8) Å^2 at 123 K. In urea (Swaminathan, Craven & McMullan, 1984*a*), there is a similar effect, except that it is three times greater in magnitude. These authors suggest that as the temperature increases, the coupling of urea molecules by H-bonding causes damping of the H-atom motion relative to a vibrating system of uncoupled rigid molecules. In alloxan, there could be a similar effect but with smaller damping because the H-bonding is much weaker.

The bond lengths and angles (Table 5) have been corrected for rigid-body librations and for the non-rigid motion of the H and O(2) atoms. The N–H bond lengths have also been corrected for anharmonic bond-stretching motion (Weber, Craven & McMullan, 1983). The corrected bond lengths in alloxan agree well with those in parabanic acid (Craven & McMullan, 1979; Swaminathan, Craven & McMullan, 1984*b*), which is a similar molecule except that it has a five-membered ring. From the values of the C–O and C–N bond lengths, there appears to be considerably less conjugation within the ureide moiety of alloxan and parabanic acid than in urea itself. Thus, comparing ureide bond lengths in alloxan with those recently determined for urea by neutron diffraction at 12, 60 and 123 K (Swaminathan *et al.*, 1984*a*), the C–O bond in alloxan is shorter [1·215 (1) *vs* 1·265 (1) Å] and the C–N bonds are longer [1·391 (1) *vs* 1·349 (2) Å]. Conjugation effects also appear to be minimal in the ketone group of alloxan, since the C(5)=O(5) bond is unusually short, 1·200 (2) Å, and the adjacent C(5)–C(6) bond is long, 1·533 (1) Å. For comparison, the corresponding bond lengths in glyoxal are 1·208 (2) and 1·525 (3) Å as determined from both microwave spectra and gas electron diffraction (Kuchitsu, Fukuyama & Morino, 1968).

Table 5. *Interatomic distances* (Å) *and angles* (°)

(*a*) Bond lengths

	Uncorrected		Corrected	
	42 K	123 K	42 K	123 K
C(2)–O(2)	1·213 (1)	1·209 (1)	1·215 (1)	1·213 (1)
C(2)–N(1)	1·388 (1)	1·388 (1)	1·390 (1)	1·391 (1)
N(1)–H(1)	1·021 (2)	1·021 (2)	1·021 (3)*	1·026 (3)*
N(1)–C(6)	1·366 (1)	1·365 (1)	1·368 (1)	1·369 (1)
C(6)–O(6)	1·214 (1)	1·212 (1)	1·216 (1)	1·215 (1)
C(6)–C(5)	1·531 (1)	1·529 (1)	1·533 (1)	1·533 (1)
C(5)–O(5)	1·197 (1)	1·198 (1)	1·199 (1)	1·201 (1)

(*b*) Bond angles†

	42 K	123 K
N(1)–C(2)–N(1)′	117·9 (1)	117·8 (1)
O(2)–C(2)–N(1)	121·1 (1)	121·1 (1)
C(2)–N(1)–H(1)	115·7 (1)	115·5 (1)
C(2)–N(1)–C(6)	126·4 (1)	126·5 (1)
H(1)–N(1)–C(6)	117·8 (1)	117·9 (1)
N(1)–C(6)–O(6)	124·0 (1)	123·9 (1)
N(1)–C(6)–C(5)	115·4 (1)	115·3 (1)
O(6)–C(6)–C(5)	120·6 (1)	120·8 (1)
C(6)–C(5)–O(5)	120·8 (1)	120·7 (1)
C(6)–C(5)–C(6)′	118·5 (1)	118·7 (1)

(*c*) Intermolecular distances (Å) and angles (°) (uncorrected)

	42 K	123 K
H(1)···O(2^{i})	2·307 (2)	2·324 (2)
H(1)···O(6^{ii})	2·338 (2)	2·352 (2)
H(1)···O(5^{iii})	2·798 (3)	2·808 (2)
N(1)···O(2^{i})	3·149 (1)	3·165 (1)
N(1)···O(6^{ii})	3·222 (1)	3·235 (1)
N(1)···O(5^{iii})	2·991 (1)	3·004 (1)
C(5)···O(6^{iv})	2·720 (1)	2·733 (1)
C(6)···O(6^{iv})	2·885 (1)	2·902 (1)
C(6)′···O(6^{iv})	2·983 (1)	2·988 (1)
O(2)···O(5^{v})	2·991 (1)	3·009 (1)
O(2)···O(6^{v})	2·887 (1)	2·904 (1)
O(2)···O(6^{vi})	3·030 (1)	3·038 (1)
N(1)–H(1)···O(2^{i})	138·80 (17)	138·80 (13)
N(1)–H(1)···O(6^{ii})	144·06 (16)	144·19 (13)
N(1)–H(1)···O(5^{iii})	90·74 (13)	90·98 (10)
O(2^{i})···H(1)···O(6^{ii})	76·85 (8)	76·78 (6)
O(5)–C(5)···O(6^{iv})	105·39 (13)	105·41 (10)
O(6)–C(6)···O(6^{iv})	110·72 (6)	110·82 (5)
O(6)′–C(6)′···O(6^{iv})	114·34 (6)	114·26 (5)

Symmetry code: (i) $\frac{1}{2}+y, -\frac{1}{2}-x, -\frac{1}{4}+z$; (ii) $-\frac{1}{2}+x, -\frac{1}{2}-y, -\frac{1}{4}-z$; (iii) $-\frac{1}{2}+y, \frac{1}{2}-x, -\frac{1}{4}+z$; (iv) $\frac{1}{2}-y, -\frac{1}{2}+x, \frac{1}{4}+z$; (v) $-1+x, -1+y, z$; (vi) $-\frac{1}{2}-y, -\frac{1}{2}+x, \frac{1}{4}+z$.

* Includes anharmonic stretching correction.

† After correction for thermal libration, bond angles are unchanged except for C(6)–C(5)–C(6)′ at 123 K, which becomes 118·6 (1)°. Atoms marked (′) have positions ($y, x, -z$). They belong to the same molecule as those listed in Table 2.

Dynamical deformation density from Fourier syntheses

The *X–N* maps (Fig. 5) are difference Fourier syntheses showing the dynamical deformation charge density for alloxan in the molecular plane. The Fourier series have amplitudes $|F_o|-|F_c|$ where F_c is the structure factor calculated for a promolecule consisting of neutral spherical atoms with atomic positional and thermal parameters determined by neutron diffraction. Atomic scattering factors assume Hartree–Fock C, N and O atoms (Cromer & Waber, 1965) and bonded spherical H atoms (Stewart, Davidson & Simpson, 1965). In Fig. 5(*a*), amplitudes $|F_o|$ and $|F_c|$ are both assigned the phase angle φ_c determined from the promolecule structure factors, F_c. In Fig. 5(*b*), details of the deformation density are enhanced as a result of assigning different phases to $|F_o|$ and $|F_c|$. Thus the amplitudes $|F_o|$ have phases φ_m, determined from the structure factors F_m for the pseudoatom model. The phases φ_m and φ_c for the two models of the structure can differ because they are unrestricted for general reflections *hkl* in the noncentrosymmetric space group $P4_12_12$. For comparison, Fig. 5(*c*) shows the difference between the charge density calculated for the pseudoatom structure (amplitudes $|F_m|$, phases φ_m) and for the promolecule structure (amplitudes $|F_c|$, phases φ_c). This is the idealized deformation density in which it is assumed that neither the amplitudes nor the phases are subject to error.

Although there is qualitative agreement among the maps in Fig. 5, the charge distributions are not easily interpreted. In each case, the Fourier series includes only reflections with $\sin\theta/\lambda < 0{\cdot}8$ Å^{-1}. Other maps with higher resolution showed the expected sharpening of the charge features, but at the expense of an

increasing noise level. Atom centers occurred in troughs of increasing depth. Also, there is the inherent limitation in $X-N$ maps that they show the deformation density smeared by the atomic thermal motion in the crystal. For a more detailed discussion, it is preferable to consider the deformation density calculated for atoms at rest, as can be obtained directly from the rigid pseudoatom model.

The distribution of pseudoatom net charges

The net charge on each pseudoatom in alloxan is given by the difference between the formal valence charge (4 for C atoms, *etc.*) and the monopole electron population parameter (p_v in Table 3). Thus in alloxan, as in parabanic acid (Craven & McMullan, 1979), the C and O atoms are neutral within experimental error, except for O(6) which has a marginal negative charge, −0·11 (3) e. This is consistent with the bond-length distribution (discussed above) in indicating that the bonding system in alloxan is only weakly conjugated. There is no evidence that the short intermolecular O=C···O distances in alloxan are the result of Coulombic attractions between oppositely charged C and O atoms.

The net atomic charges in alloxan are greatest for the N–H group, in which the N atom is significantly negative, −0·50 (4) e, and the H atom is positive, +0·34 (4) e.* In crystal structures such as phosphorylethanolamine (Swaminathan & Craven, 1984), γ-aminobutyric acid (Craven & Weber, 1983) and imidazole (Epstein *et al.*, 1982), it has been noted that the H atoms of N–H and O–H groups are positively charged, whereas those of C–H groups are nearly neutral. This helps to explain why C–H groups are not usually H-bonded. It is of interest that in alloxan, the charge distribution of the N–H group resembles other N–H groups, rather than a C–H group, although in this case, the H-bonding of the N–H group is very weak.

* It must be remembered that the magnitude of this charge separation depends on the radial exponents (α) which are assumed in describing the charge density. In this case, standard α values were used (Hehre *et al.*, 1969).

Static deformation density from the pseudoatom model

Because of the good agreement between the atomic thermal parameters obtained at 123 K from X-ray and neutron diffraction (Table 2*b*), we believe that the thermal motion in alloxan has been well determined. Under similar circumstances, in the case of urea (Swaminathan, Craven, Spackman & Stewart, 1984), a comparison of experimental and theoretical results has shown that Stewart's (1976) pseudoatom model satisfactorily represents the static deformation density deconvoluted from the thermal motion.

In alloxan, the deformation density for the ureide group is similar to that of urea itself, except that the features are reduced in magnitude. Thus, along the C–N bond, the maximum positive density is 0·7 (1) e Å^{-3} in alloxan and 0·9 (1) e Å^{-3} in urea (Swaminathan *et al.*, 1984*a*). Also, in alloxan there is negative density along the C–N bond (Fig. 6*a*) which does not occur in urea. These differences are consistent with the C–N bonding being shorter in urea [1·391 (1) *vs* 1·348 (2) Å]. It is difficult to find similar correlations involving the C–O bond lengths because of the greater complexity in the deformation density of the carbonyl group. In this group, the most significant difference occurs in the paired lobes which flank the O atom in the molecular plane, the maximum values being 0·6 (2) e Å^{-3} in alloxan and 1·5 (3) e Å^{-3} in urea. The net deformation density along the C–O bond comes from the offsetting effects of an excess of electronic charge near the C atom and a deficiency

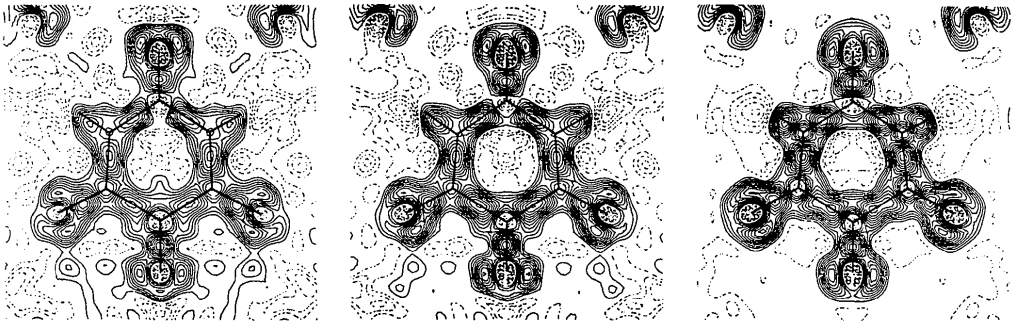

(*a*) (*b*) (*c*)

Fig. 5. Fourier syntheses ($X-N$) showing the dynamic deformation charge density in the molecular plane. The molecule is oriented as in Fig. 4. Reflections with $\sin\theta/\lambda \le 0{\cdot}8$ Å^{-1} are included. Contours are at intervals of 0·05 e Å^{-3}, with the zero contour omitted. (*a*) Map of (ρ_o-ρ_c) where subscript *o* refers to the electron density based on the observed structure amplitudes and *c* refers to the electron density for the promolecule structure. The phases φ_c are from the promolecule structure. (*b*) Map of ($\rho_o - \rho_c$) where ρ_o has phases φ_m from the pseudoatom model and ρ_c has phases φ_c as in (*a*). (*c*) Map of (ρ_m-ρ_c) which is the idealized difference between the electron density of the pseudoatom and promolecule structures.

near the O atom. This polarization is noticeable in urea and the ureide group in alloxan, but is reduced in the other carbonyl groups of alloxan. In the regions above and below the molecular plane, there are lobes of charge depletion at both the C and O atoms (Fig. 7*a*). This appears to be characteristic of the deformation density at the C atom of all carbonyl groups.* At C(5) in alloxan, the charge depletion occurs along the directions of the two shortest (2·73 Å) intermolecular C···O distances and may be important for understanding why these interactions occur.

At the H atom, there is a strong dipole deformation which increases the charge density in the N–H bond and depletes charge from the region of the H-bonding interaction (Fig. 8*a*). The negative density near the H atom extends towards O(2^{i}), imparting asymmetry to the weak bifurcated interaction.

The electrostatic potential

The pseudoatom model has been used to map the electrostatic potential for an isolated alloxan molecule (Figs. 6*b*, 7*c*, 8*c*), and for discrete groups of alloxan molecules arranged in the same way as in the crystal structure (Figs. 7*b*, 8*b*). In these maps, the negative regions are those of low potential energy for a positive unit charge as probe.

Within the molecular plane (Fig. 6*b*), the most striking feature in the potential for the isolated molecule is the diffuseness of the positive region around the H atom. There are also less pronounced negative regions surrounding the O atoms, which are most noticeable for O(2) [$-100(33)$ kJ mol^{-1}]. Because of these features in the electrostatic potential, a weak attractive interaction should occur when the O atoms are brought into the H-bonding configuration (Fig. 8). From Fig. 8(*c*), it is calculated that a point charge of 0·1 e at a distance 1·5 Å from the H atom would have a potential energy -12 kJ mol^{-1} if it were placed along the line H···O(2^{i}) and -4 kJ mol^{-1} if it were along H···O(6^{ii}). It is noteworthy that the interatomic distances and angles in the bifurcated H-bond indicate a nearly symmetric interaction, while from the electrostatic properties it appears that the N–H group interacts more strongly with O(2^{i}) than with O(6^{ii}). In Fig. 8(*b*), which shows the electrostatic potential calculated for a discrete group of three H-bonded molecules, the negative potential from the O atoms is cancelled by the positive potential from the H atom. Along both the H···O lines, there are saddle points of nearly zero potential.

Other regions near the alloxan molecule in which the electrostatic potential is of particular interest are along the directions of the short O=C···O intermolecular distances (Fig. 7). In the isolated molecule (Fig. 7*c*), the positive potential on either side of the molecular plane is considerably more extensive at C(5) than at the other carbonyl C atoms. The effect is due to the higher multipole terms in the charge-density distribution, because the electrostatic potential calculated only with monopole terms shows a contraction at the carbonyl C atoms, with C(5) indistinguishable from the others. The short intermolecular C···O distances at C(5) appear to be derived primarily from the deshielding of the carbonyl C-atom nucleus, thus allowing close approach of the weakly electronegative O(6) atoms on either side of the molecular plane. When three alloxan molecules are brought together as in Fig. 7(*b*), saddle points of nearly zero potential are formed along the lines C(5)···O(6). However, these C···O interactions can be only weakly attractive. Although atom O(6) carries a small negative net charge of $-0·11(3)$ e, the electrostatic potential around O(6) in the isolated molecule is almost zero.

As pointed out by Craven & McMullan (1979), the C···O distances in alloxan and in several other crystal structures (Bürgi *et al.*, 1974) could be regarded as normal if a smaller van der Waals radius for the carbonyl C atom were to be assumed. The currently accepted value (1·7 Å), as derived from the crystal structure of graphite, is suitable for the van der Waals radius of an aromatic C atom. For the carbonyl C atom, a value smaller by at least 0·2 Å is recommended (1·5 Å for crystal structures at room temperature). This would be consistent with the observed internuclear C···O distances and could be justified in terms of the depletion of electronic charge at the carbonyl C atom from above and below the molecular plane.

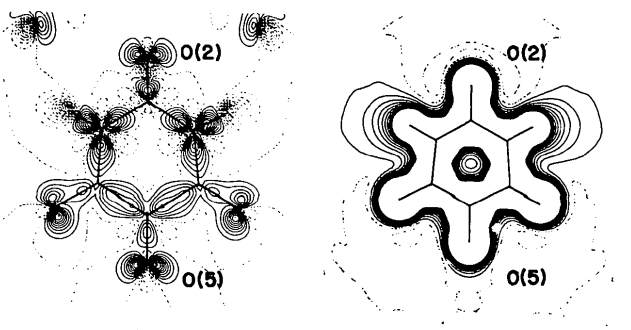

(*a*) (*b*)

Fig. 6. Electrostatic properties of alloxan in the molecular plane as computed from the pseudoatom model with atoms at rest. (*a*) Deformation charge density in the crystal structure. Contours are at intervals 0·1 e Å^{-3}, with zero as the first dotted contour. (*b*) Total electrostatic potential for an isolated molecule. Contours are at intervals 0·05 e Å^{-1} ≡ 69·5 kJ mol^{-1} corresponding to about one e.s.d.

* However, the deformation density at the O atom is not always as described here. In the carbonyl groups of acetamide (Berkovitch-Yellin, Leiserowitz & Nader, 1977), formamide (Stevens, 1978), and barbital (Craven, Fox & Weber, 1982), features in the O-atom deformation density are rotated about the C–O bond so that the maxima occur above and below the amide plane and the minima are within the plane. The effect is yet to be explained.

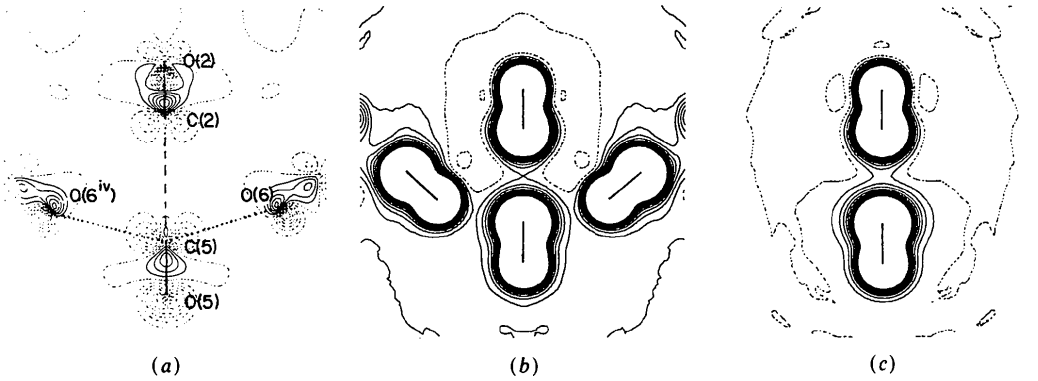

Fig. 7. Electrostatic properties in the section normal to the molecular plane and passing through the axis O(2)C(2)C(5)O(5). Atoms O(6), which form the shortest C···O intermolecular distances (2·73 Å), are ±0·1 Å from this plane. Maps are computed from the pseudoatom model with atoms at rest. (*a*) The deformation charge density in the crystal structure. Contours are at intervals 0·1 e Å^{-3}. (*b*) The total electrostatic potential for a group of three molecules arranged as in (*a*). Line segments join atoms of C–O groups. Contours are at intervals 0·05 e Å^{-1} ≡ 69·5 kJ mol^{-1}. (*c*) The total electrostatic potential for the isolated central molecule in (*a*) and (*b*).

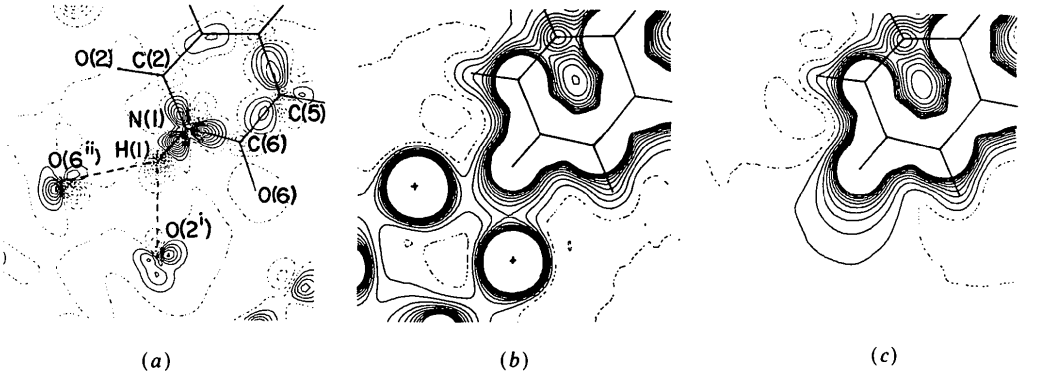

Fig. 8. Electrostatic properties in the section of the best least-squares plane through atoms N(1), H(1), O(2^{i}) and O(6^{ii}) which are involved in the weak bifurcated H-bond. Maps are computed from the pseudoatom model with atoms at rest. (*a*) The deformation charge density in the crystal structure. Contours are at intervals 0·1 e Å^{-3}. (*b*) Total electrostatic potential for the group of three molecules which form the H-bond. Contours are at intervals 0·05 e Å^{-1} ≡ 69·5 kJ mol^{-1}. (*c*) Total electrostatic potential for the isolated molecule which is outlined.

The neutron data collection and the ensuing structure refinements were carried out at the Brookhaven National Laboratory, under contract with the US Department of Energy. The work was supported by NIH Grant GM-22548. We are grateful to Dr R. F. Stewart for providing some details of the procedure for deriving the electrostatic potential from the pseudoatom model. We also thank Mr Joseph Henriques and Mrs Joan Klinger for technical assistance.

References

BECKER, P. J. & COPPENS, P. (1974). *Acta Cryst.* **A30**, 129-147.

BERKOVITCH-YELLIN, Z., LEISEROWITZ, L. & NADER, F. (1977). *Acta Cryst.* **B33**, 3670-3677.

BLESSING, R. H., COPPENS, P. & BECKER, P. (1974). *J. Appl. Cryst.* **7**, 480-492.

BOLTON, W. (1964*a*). *Acta Cryst.* **17**, 147-152.

BOLTON, W. (1964*b*). *Nature (London)*, **201**, 987-989.

BÜRGI, H. B., DUNITZ, J. D. & SHEFTER, E. (1974). *Acta Cryst.* **B30**, 1517-1527.

BUSING, W. R., MARTIN, K. O. & LEVY, H. A. (1962). *ORFLS.* Report ORNL-TM-305. Oak Ridge National Laboratory, Tennessee.

CLEMENTI, E. (1965). *IBM J. Res. Dev. Suppl.* **9**, 2.

CRAVEN, B. M., FOX, R. O. JR & WEBER, H.-P. (1982). *Acta Cryst.* **B38**, 1942-1952.

CRAVEN, B. M. & HE, X. M. (1982). *Programs for Thermal Motion Analysis*, Tech. Rep. Crystallography Department, Univ. of Pittsburgh.

CRAVEN, B. M. & MCMULLAN, R. K. (1979). *Acta Cryst.* **B35**, 934-945.

CRAVEN, B. M. & TAKEI, W. J. (1964). *Acta Cryst.* **17**, 417-420.

CRAVEN, B. M. & WEBER, H.-P. (1981). *The POP Least-Squares Refinement Procedure.* Tech. Rep. Crystallography Department, Univ. of Pittsburgh.

CRAVEN, B. M. & WEBER, H.-P. (1983). *Acta Cryst.* **B39**, 743-748.

CROMER, D. T. & WABER, J. T. (1965). *Acta Cryst.* **18**, 104-109.

CROMER, D. T., WABER, J. T. & IBERS, J. A. (1974). *International Tables for X-ray Crystallography*, Vol. IV, pp. 148-151. Birmingham: Kynoch Press.

EPSTEIN, J., RUBLE, J. R. & CRAVEN, B. M. (1982). *Acta Cryst.* B**38**, 140-149.
HAMILTON, W. C. & IBERS, J. A. (1968). *Hydrogen Bonding in Solids.* New York: Benjamin.
HANSEN, N. K. & COPPENS, P. (1978). *Acta Cryst.* A**34**, 909-921.
HE, X. M. (1983). *The MOLPOT Computer Program.* Tech. Rep. Department of Crystallography, Univ. of Pittsburgh.
HEHRE, W. J., STEWART, R. F. & POPLE, J. A. (1969). *J. Chem. Phys.* **51**, 2657-2664.
HUTCHINGS, M. T., SCHULHOF, M. P. & GUGGENHEIM, H. J. (1972). *Phys. Rev. B*, **5**, 154-168.
JEFFREY, G. A. & MALUSZYNSKA, H. (1982). *Int. J. Biol. Macromol.* **4**, 173-185.
JOHNSON, C. K. & LEVY, H. A. (1974). *International Tables for X-ray Crystallography*, Vol. IV, pp. 311-336. Birmingham: Kynoch Press.
KOESTER, L. (1977). *Neutron Physics*, edited by G. HOHLER, p. 1. Berlin: Springer.
KUCHITSU, K., FUKUYAMA, T. & MORINO, Y. (1968). *J. Mol. Struct.* **1**, 463-479.
LEHMANN, M. S. & LARSEN, F. K. (1974). *Acta Cryst.* A**30**, 580-584.
MCMULLAN, R. K. & KOETZLE, T. F. (1980). Unpublished.
MEULENAER, J. DE & TOMPA, H. (1965). *Acta Cryst.* **19**, 1014-1018.
MOOTZ, D. & JEFFREY, G. A. (1965). *Acta Cryst.* **19**, 717-725.
PAULING, L. (1960). *The Nature of the Chemical Bond.* Ithaca: Cornell Univ. Press.
PROUT, C. K. & WALLWORK, S. C. (1966). *Acta Cryst.* **21**, 449-450.
PULLMAN, B. (1964). *Acta Cryst.* **17**, 1074-1075.
SCHOMAKER, V. & TRUEBLOOD, K. N. (1968). *Acta Cryst.* B**24**, 63-76.
SINGH, C. (1960). *Acta Cryst.* **13**, 1036.
STEVENS, E. D. (1978). *Acta Cryst.* B**34**, 544-555.
STEWART, R. F. (1970). *J. Chem. Phys.* **57**, 1664-1668.
STEWART, R. F. (1976). *Acta Cryst.* A**32**, 565-574.
STEWART, R. F., DAVIDSON, E. R. & SIMPSON, W. T. (1965). *J. Chem. Phys.* **42**, 3175-3187.
SWAMINATHAN, S. & CRAVEN, B. M. (1984). *Acta Cryst.* B**40**, 511-518.
SWAMINATHAN, S., CRAVEN, B. M. & MCMULLAN, R. K. (1984*a*). *Acta Cryst.* B**40**, 300-306.
SWAMINATHAN, S., CRAVEN, B. M. & MCMULLAN, R. D. (1984*b*). *Acta Cryst.* Submitted.
SWAMINATHAN, S., CRAVEN, B. M., SPACKMAN, M. & STEWART, R. F. (1984). *Acta Cryst.* B**40**, 398-404.
TEMPLETON, L. K. & TEMPLETON, D. H. (1973). *Abstr. Am. Crystallogr. Assoc. Meet.*, Storrs, CT, p. 143.
WEBER, H.-P., CRAVEN, B. M. & MCMULLAN, R. K. (1983). *Acta Cryst.* B**39**, 360-366.

Acta Cryst. (1985). B**41**, 122-131

Structural Investigations of Phosphorus–Nitrogen Compounds. 1. The Structures of Three Monospiro Compounds: $N_3P_3[O(CH_2)_2O]Cl_4$, $N_3P_3[O(CH_2)_3O]Cl_4$ and $N_3P_3[O(CH_2)_4O]Cl_4$. The Relationship of OPO Bond Angles in PO_2N_2 Tetrahedra with ^{31}P Chemical Shifts*

BY SORAB R. CONTRACTOR,† MICHAEL B. HURSTHOUSE,‡ LEYLÂ S. SHAW (NEÉ GÖZEN),†‡ ROBERT A. SHAW†§ AND HAMZA YILMAZ†

Department of Chemistry, Birkbeck College (University of London), Malet Street, London WC1E 7HX and Department of Chemistry, Queen Mary College (University of London), Mile End Road, London E1 4NS, England

(*Received* 18 *April* 1984; *accepted* 3 *September* 1984)

Abstract

The crystal structures of three dioxyalkane monospiro compounds {2,2-ethylenedioxy-4,4,6,6-tetrachlorocyclotriphosphazatriene, $N_3P_3[O(CH_2)_2O]Cl_4$ (1), 2,2-trimethylenedioxy-4,4,6,6-tetrachlorocyclotriphosphazatriene, $N_3P_3[O(CH_2)_3O]Cl_4$ (2), and 2,2-tetramethylenedioxy-4,4,6,6-tetrachlorocyclotriphosphazatriene, $N_3P_3[O(CH_2)_4O]Cl_4$ (3)} have been determined by X-ray analysis. [Crystal data: (1): triclinic, $P\bar{1}$, $a = 7{\cdot}763\ (2)$, $b = 8{\cdot}008\ (2)$, $c = 10{\cdot}352\ (3)$ Å, $\alpha = 99{\cdot}38\ (2)$, $\beta = 93{\cdot}95\ (2)$, $\gamma = 110{\cdot}83\ (2)°$, $Z = 2$; (2): orthorhombic, $Cmc2_1$, $a = 10{\cdot}650\ (2)$, $b = 13{\cdot}457\ (2)$, $c = 8{\cdot}833\ (2)$ Å, $Z = 4$; (3): monoclinic, $C2/c$, $a = 10{\cdot}733\ (3)$, $b = 13{\cdot}646\ (3)$, $c = 9{\cdot}099\ (1)$ Å, $\beta = 93{\cdot}39\ (2)°$, $Z = 4$.] For structure solutions direct methods [*SHELX*76 (1), *SHELX*84 (2)] and Patterson methods (3) were used. Full-matrix least-squares refinements led to R values of 5·6% for (1), 3·3% for (2) and 4·1% for (3) using 2052, 588, and 1324 unique reflections respectively [$F_o > 3\sigma(F_o)$]. The cyclotriphosphazatriene moiety is essentially planar in all three compounds. The bond lengths and angles of this ring show the expected effects of replacing two Cl atoms by the more electron-releasing alkoxy groups. However, the data show no

*Presented in part at the International Conference on Phosphorus Chemistry, Nice, France, September 1983. [The chemical nomenclature used throughout this paper conforms to that established by Shaw, Fitzsimmons & Smith (1962) and differs from current IUPAC recommendations.]

† Birkbeck College.
‡ Queen Mary College.
§ Author for correspondence.

0108-7681/85/020122-10$01.50